DETERMINISTIC WALKS IN QUENCHED RANDOM ENVIRONMENTS OF CHAOTIC MAPS

TAPIO SIMULA AND MIKKO STENLUND

Abstract. This paper concerns the propagation of particles through a quenched random medium. In the one- and two-dimensional models considered, the local dynamics is given by expanding circle maps and hyperbolic toral automorphisms, respectively. The particle motion in both models is chaotic and found to fluctuate about a linear drift. In the proper scaling limit, the cumulative distribution function of the fluctuations converges to a Gaussian one with system dependent variance while the density function shows no convergence to any function. We have verified our analytical results using extreme precision numerical computations.

1. Introduction

Variants of a mechanical model now widely known as the Lorentz gas have occupied the minds of scientists for more than a century. Initially proposed by Lorentz [Lo] in 1905 to describe the motion of an electron in a metallic crystal, the model consists of fixed, dispersing, scatterers in $\mathbb{R}^d$ and a free point particle that bounces elastically off the scatterers upon collisions.

If the lattice of scatterers is periodic, the model is also referred to as Sinai Billiards after Sinai, who proved [Si] that the system (with $d = 2$) is ergodic if the free path of the particle is bounded. In the latter case it was also proved that, in a suitable scaling limit, the motion of the particle is Brownian [BuSi]. Sinai's work can be considered the first rigorous proof of Boltzmann's Ergodic Hypothesis in a system that resembles a real-world physical system.

The Lorentz gas exhibits a great deal of complexity. One example is the lack of smoothness of the dynamics caused by tangential collisions of the particle with the scatterers. Another one, the presence of recollisions, is a source of serious statistical difficulties that have not

Date: April 2, 2009.

2000 *Mathematics Subject Classification.* 60F05; 37D20, 82C41, 82D30.

Key words and phrases. Random environments, hyperbolic dynamical systems, Gaussian fluctuations, Lorentz gas.

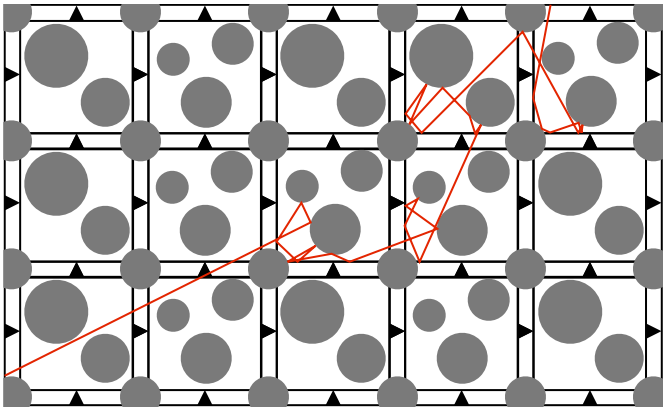

FIGURE 1. Schematic diagram illustrating the qualitative features of our two-dimensional model. The medium is composed of two different types of square cells separated by walls which allow particles to pass only in the direction of the arrowheads. The zig-zag line shows a path of a particle through the medium.

been overcome in the study of the aperiodic Lorentz gas. For more background, see [Ta, Sz, ChMa, ChDo] and the references therein.

Our study concerns an idealization of the aperiodic Lorentz gas with semipermeable walls illustrated in Figure 1. In each cell, there is a configuration of scatterers drawn independently from the same probability distribution. In our case, the distribution is Bernoulli, so that there are two possible configurations to choose from inside each cell. As an important aspect, the environment thus obtained is quenched; once the scatterer configurations have been randomly chosen, they are frozen for good, and the only randomness that remains is in the initial data of the particle. Between the cells are semipermeable walls that allow the particle to pass through from left to right and from bottom to top, as shown by the arrowheads, but not in the opposite directions. This model may be thought of as describing the propagation of particles in an anisotropic medium.

Notice that, as a significant simplification, there is no recurrence; once a particle leaves a cell, it never returns to the same cell again. Yet a particle *can* occupy a single cell for an arbitrarily long time before moving on to a neighboring one—albeit a long occupation time has a small probability. Moreover, where, when, and in which direction the particle exits a cell depends heavily on the scatterer configuration inside the cell, in addition to the position and direction of the particle at entry. Inside each cell, the dynamics is chaotic and hyperbolic.

In our one- and two-dimensional idealizations, the billiard dynamics is replaced by discrete dynamical systems acting in each cell. In other words, acting on the particle's current position by a map associated to the current cell gives its position one time unit later. In dimension one the maps associated to the cells are smooth, uniformly expanding, maps while in dimension two they are smooth, uniformly hyperbolic, maps with one expanding and one contracting dimension. Such maps retain the chaotic and hyperbolic nature of the problem. A closely related model has been studied in [AySt, AyLiSt].

Our objective is to understand certain statistical properties of the motion. More precisely, we are interested in how the particle distribution evolves with time when the initial distribution is uniform and supported on one initial cell. We make several analytical propositions, which we verify numerically. We show that, on the average, the particles follow a linear drift and that, after taking a suitable scaling limit, the cumulative distribution of the fluctuations about the mean is Gaussian. Moreover, the drift and variance are the same for (almost) all environments drawn from the same distribution. Nevertheless, the particle distribution shows rapid oscillations due to the quenched environment. In particular, the density function does *not* converge to that of a normal distribution. In fact, it does not converge at all in the aforementioned scaling limit.

Acknowledgements. We are indebted to Arvind Ayyer and Joel Lebowitz for stimulating discussions. Tapio Simula is supported by the Japan Society for the Promotion of Science Postdoctoral Fellowship for Foreign Researchers. Mikko Stenlund is partially supported by a fellowship from the Academy of Finland.

2. One-dimensional model: expanding maps on the circle

2.1. **Preliminaries.** Imagine tiling the nonnegative half line $[0,\infty)$ so that each interval—or tile—$I_k = [k, k+1)$ with $k \in \mathbb{N}$ carries a label $\omega(k)$ that equals either 0 or 1. Such a tiling can be realized by flipping a coin for each k and encoding the outcomes in a sequence $\omega = (\omega(0), \omega(1), \dots) \in \{0,1\}^{\mathbb{N}}$ called the *environment*. The coin could be balanced but the tosses are independent, with $\mathrm{Prob}(\omega(k) = i) = p_i$ for all k. In the following, $\mathbb{P}_{p_0}$ will stand for the corresponding probability measure on the space of Bernoulli sequences ω. In each experiment we freeze the environment—meaning that we work with one *fixed* sequence ω at a time.

The dynamics in our model is generated by the following definitions. Let v_n be the position of the particle and x_n its decimal value.

Furthermore, suppose $A_0, A_1 \in \{2, 3, \dots\}$ and define the circle maps $T_i(x) = A_i x \mod 1$. An experiment comprises iterating the map on $\mathbb{R}_+ \times \mathbb{S}^1$ given by $(v_{n+1}, x_{n+1}) = (v_n + A_{\omega([v_n])} x_n - x_n, T_{\omega([v_n])}(x_n))$, where $[v_n]$ is the integer part of v_n and $\omega([v_n])$ is the corresponding component of ω. Our initial condition is $(v_0, x_0) = (x, x)$, with $x \in [0, 1)$. Let $\mathbf{P}$ denote the Lebesgue measure (*i.e.*, the uniform probability distribution) on the circle $\mathbb{S}^1$ and $\mathbf{E}$ the corresponding expectation.

The model thus describes the deterministic motion of a particle in a randomly chosen, but fixed, environment. In probability jargon, the particle performs a deterministic walk in a quenched random environment. The *map* determining v_{n+1} depends on the tile $I_{[v_n]}$ the particle is in through the label $\omega([v_n])$ of the tile. That is, the motion of the particle is guided by the *a priori* chosen environment.

The maps we have chosen are of the simplest kind, which helps numerical and analytical computations. This is not to say that the resulting dynamics is exceptional among more general expanding maps. On the contrary, the qualitative features of the dynamics should be universal within the classes of maps mentioned in the introduction.

Example 1. *A concrete example is obtained by choosing* $A_0 = 2$*,* $A_1 = 3$*, and* $p_0 = p_1 = \frac{1}{2}$*.*

For each x (and ω) we have to *compute* which map the symbol $A_{\omega([v_1])}$ stands for. Each v_n ($n \geq 2$) is generically a piecewise affine function of x and the number of discontinuities grows exponentially with n. We anticipate that, for large values of n, v_n behaves statistically (in the weak sense) as

$$v_n \approx \mathcal{N}(nD, n\sigma^2), \tag{1}$$

where D is a deterministic number called the *drift* and $\mathcal{N}(nD, n\sigma^2)$ stands for a real-valued, normally distributed, random variable with mean nD and variance $n\sigma^2$. In principle, D and σ^2 could depend on the environment ω, but remarkably it turns out that they do not, as long as the environment is *typical*. By typicality we mean that ω belongs to a set whose $\mathbb{P}_{p_0}$-probability is one and whose elements enjoy good statistical properties such as the convergence of $\frac{1}{n}\#\{k < n \,|\, \omega(k) = 0\}$ to the limit p_0.

It is reasonable to expect that the limit

$$\lim_{n\to\infty} \frac{v_n(x)}{n}$$

exists and has the same value for almost all x [1]. Thus, we are led to conclude that

$$D = \mathbf{E}\left(\lim_{n\to\infty} \frac{v_n(x)}{n}\right) = \lim_{n\to\infty} \frac{1}{n}\mathbf{E}(v_n(x))\,.$$

The final equality follows from the bounded convergence theorem.

If the initial condition $x \in [0,1)$ is chosen uniformly at random, v_n can be regarded as a random variable. Let us consider the (asymptotically) centered random variable

$$X_n = v_n - nD,$$

which measures the fluctuations of v_n relative to the linear drift. Provided (1) is true, X_n is approximately Gaussian with variance $n\sigma^2$. More precisely, we would like to know if $\frac{1}{\sqrt{n}}X_n$ converges in distribution to $\mathcal{N}(0,\sigma^2)$. By definition, this means that, for any fixed $y \in \mathbb{R}$,

$$\lim_{n\to\infty} \mathbf{P}\left(\frac{1}{\sqrt{n}}X_n \le y\right) = \frac{1}{\sqrt{2\pi}\sigma}\int_{-\infty}^{y} e^{-s^2/2\sigma^2}\,ds.$$

2.2. **Markov partition.** We next reduce the deterministic walk in a random environment to a random walk in a random (still quenched) environment which is easier to treat. This can be done using a Markov property of the tiling that allows us, in the statistical sense, to ignore the exact position of the particle and only keep track of the tile it is occupying.

Let $[\,\cdot\,]$ denote the integer part of a number. If we define

$$V_n = [v_n] \quad \text{and} \quad x_n = v_n - [v_n], \tag{2}$$

then the earlier dynamics with the initial condition $(v_0, x_0) = (x, x)$ is equivalent to

$$\begin{aligned} V_{n+1} &= V_n + \left[A_{\omega(V_n)}x_n\right] \\ x_{n+1} &= A_{\omega(V_n)}x_n - \left[A_{\omega(V_n)}x_n\right]. \end{aligned} \tag{3}$$

Recall our convention $[0,\infty) = \bigcup_{k=0}^{\infty} I_k$, where $I_k = [k, k+1)$ is called a tile. Suppose now that $v_n \in I_k$. This is equivalent to $V_n = k$. As before, we are interested in the probability distribution of v_n when x is chosen at random, but this time only at the level of tiles. Notice that $v_n = [v_n] + \{v_n\}$, where $0 \le \{v_n\} < 1$. Therefore, $v_n/\sqrt{n}$ and $[v_n]/\sqrt{n}$ differ by at most $1/\sqrt{n}$, so their asymptotic distributions are the same (and in fact very close to each other even for moderate values of n). More precisely, we wish to know the probability distribution

[1] This cannot hold for all x. For instance, if $x = \frac{1}{kA_{\omega(0)}}$, then $1 = v_k = v_{k+1} = \dots$ and the process stops.

of V_n. This is the probability vector $\rho^{(n)} = (\rho_0^{(n)}, \rho_1^{(n)}, \dots)$ where the numbers

$$\rho_k^{(n)} = \mathbf{P}(V_n = k)$$

are such that $\sum_{k=0}^{\infty} \rho_k^{(n)} = 1$.

We now consider the dynamical system being initialized with the condition $(v_0, x_0) = (x, x)$, where $x \in [0, 1)$ is a uniformly distributed random variable. Since each $A_i I_k$ is exactly the union of a few of the intervals $I_{k'}$[2], the collection $\{I_k\}$ is a simultaneous Markov partition for the two maps. We then obtain the Markov property

$$\mathbf{P}(V_n = k_n \,|\, V_{n-1} = k_{n-1}, \dots, V_0 = k_0) \equiv \mathbf{P}(V_n = k_n \,|\, V_{n-1} = k_{n-1})$$

for admissible histories (in particular $k_0 = 0$). Thus, the statistics of V_n is precisely described by a time-homogeneous Markov chain on the countably infinite state space $\mathbb{N}$ with the transition probabilities

$$\gamma_{k \to k+l} = \begin{cases} \mathbf{P}(v_{n+1} \in I_{k+l} \,|\, v_n \in I_k) = \frac{1}{A_{\omega(k)}} & \text{if} \quad l \in \{0, 1, \dots, A_{\omega(k)} - 1\}, \\ 0 & \text{otherwise} \end{cases}$$

and initial distribution

$$\rho^{(0)} = (1, 0, 0, \dots).$$

Notice that the above holds for any environment, ω, but the resulting Markov chain does depend on the choice of ω.

Defining the transition matrix $\Gamma = (\gamma_{k \to k'})_{k,k'}$, $\rho^{(n)} = \rho^{(n-1)}\Gamma$. Thus,

$$\rho^{(n)} = \rho^{(0)}\Gamma^n \tag{4}$$

for an arbitrary initial distribution. In principle, (4) provides us with complete statistical understanding of the dynamics. For instance, the drift can be expressed as

$$D = \lim_{n \to \infty} \frac{1}{n} \mathbf{E}(v_n) = \lim_{n \to \infty} \frac{1}{n} \mathbf{E}(V_n) = \lim_{n \to \infty} \frac{1}{n} \sum_{k=0}^{\infty} k \rho_k^{(n)}.$$

In practice, calculating Γ^n for large values of n is difficult.

2.3. **Drift and variance.** For each $(i, j) \in \{0, 1\}^2$ the transition probability at time n from a tile labeled i to a tile labeled j is

$$\alpha_{ij}(n) = \mathbf{P}(\omega(V_{n+1}) = j \,|\, \omega(V_n) = i).$$

The analysis of this quantity is subtle, because it depends on the tiling. For instance, if $\omega = (0, 0, \dots)$, then $\mathbf{P}(\omega(V_{n+1}) = 0 \,|\, \omega(V_n) = 0) = 1$.

[2] A_i maps $\left[k + \frac{l}{A_i}, k + \frac{l+1}{A_i}\right)$ affinely onto $[k + l, k + l + 1)$.

The conditional probability $\mathbf{P} \times \mathbb{P}_{p_0}(\omega(V_1) = j \,|\, \omega(V_0) = i)$ equals

$$\alpha^*_{ij} = \delta_{ij}\left(\frac{1}{A_i} + \left(1 - \frac{1}{A_i}\right)p_i\right) + (1 - \delta_{ij})\left(1 - \frac{1}{A_i}\right)p_j,$$

because the elements $\omega(k)$ of the tiling are independent. Here p_i is the Bernoulli probability of getting an i in the tiling. We think of α^*_{ij} as an effective transition probability which only depends on the statistical properties of the tiling.

As n increases, the position of the particle at time n depends on the tiling on an increasing subinterval of $[0, \infty)$ and should therefore reflect increasingly the statistics of the tiling instead of its local details. We therefore expect the actual transition probability $\alpha_{ij}(n)$ to converge to the effective value α^*_{ij} with increasing time,

$$\lim_{n\to\infty} \alpha_{ij}(n) = \alpha^*_{ij}.$$

Despite this is not a rigorous statement we will build our analysis on it and show that it leads to precise predictions about the process.

Moreover,

$$\lim_{n\to\infty} (\alpha^*)^n = \begin{pmatrix} p & 1-p \\ p & 1-p \end{pmatrix} \tag{5}$$

for a $p \in (0, 1)$ that can be found by diagonalizing α^* or by solving the equilibrium equation $(p, 1-p)\alpha^* = (p, 1-p)$:

$$p = \frac{p_0\left(1 - \frac{1}{A_1}\right)}{1 - p_1\frac{1}{A_0} - p_0\frac{1}{A_1}} = \frac{p_0 A_0(A_1 - 1)}{A_0A_1 - p_1A_1 - p_0A_0}.$$

For instance, in the case of Example 1 we obtain $p = \frac{4}{7}$.

Notice that, for any probability vector $(q, 1-q)$,

$$(q, 1-q) \lim_{n\to\infty} (\alpha^*)^n = (p, 1-p).$$

The probability vector

$$(q, 1-q)\prod_{n=0}^{k} \alpha(n) = (q(k), 1 - q(k))$$

will converge to some $(q^*, 1-q^*)$, because $\alpha(n) \to \alpha^*$. In fact,

$$\begin{aligned}\lim_{N\to\infty} (q, 1-q)\prod_{n=0}^{2N} \alpha(n) &= \lim_{N\to\infty} (q(N), 1 - q(N)) \prod_{n=N+1}^{2N} \alpha(n) \\ &= (q^*, 1-q^*) \lim_{N\to\infty} (\alpha^*)^N = (p, 1-p),\end{aligned}$$

as $N \to \infty$.

We interpret the result above so that $\mathbf{P}(\omega(V_n) = 0) \to p$ and $\mathbf{P}(\omega(V_n) = 1) \to 1 - p$ as $n \to \infty$. That is, along a given (typical) trajectory, the fraction of time the particle spends in a tile labeled 0 is p:

$$\lim_{n\to\infty} \frac{\#\{k < n \,|\, \omega(V_k) = 0\}}{n} = p. \tag{6}$$

Notice that p does not depend on the (typical) tiling.

2.3.1. *Drift.* Define the jumps $\xi_i = V_i - V_{i-1}$ $(i \geq 1)$. Then $V_n = \sum_{i=1}^n \xi_i$. We also denote $\xi^{(j)}$ a random variable that takes values in $\{0, \dots, A_j - 1\}$ with uniform distribution. For a (typical) tiling,

$$\begin{aligned} D = \lim_{n\to\infty} \frac{\mathbf{E}(V_n)}{n} &= \lim_{n\to\infty} \frac{\sum_{i=1}^n \mathbf{E}(\xi_i)}{n} = p\mathbf{E}(\xi^{(0)}) + (1-p)\mathbf{E}(\xi^{(1)}) \\ &= p\frac{A_0 - 1}{2} + (1-p)\frac{A_1 - 1}{2} = \frac{pA_0 + (1-p)A_1 - 1}{2}. \end{aligned}$$

Numerical results such as shown in Figure 2 lead us to conclude that $\lim_{n\to\infty} \frac{V_n}{n} = D$ also for individual trajectories. In the case of Example 1, $D = \frac{5}{7}$.

2.3.2. *Variance.* The variance is

$$\sigma^2 = \lim_{n\to\infty} \operatorname{Var}\left(\frac{X_n}{\sqrt{n}}\right) = \lim_{n\to\infty} \frac{\operatorname{Var}(V_n)}{n}.$$

Let us assume $A_0 \leq A_1$ and study the process $W_n = \sum_{i=1}^n \zeta_i$ having the i.i.d. increments ζ_i whose distribution is $\operatorname{Prob}(\zeta_1 = k) = \frac{p}{A_0} + \frac{1-p}{A_1}$ if $0 \leq k < A_0$ and $\operatorname{Prob}(\zeta_1 = k) = \frac{1-p}{A_1}$ if $A_0 \leq k < A_1$. The increments have been chosen so that W_n mimics V_n as closely as possible. For instance, staying in the same tile ($\zeta_1 = 0$) has probability $\frac{p}{A_0} + \frac{1-p}{A_1}$, where p is the probability of being in a tile labeled 0 and $\frac{1}{A_0}$ is the probability of staying in that tile, while the second term accounts similarly for the case of label 1. Then $\operatorname{Mean}(W_n) = n \operatorname{Mean}(\zeta_1) = nD$. Setting $K(m) = \sum_{k=0}^{m-1} k^2 = \frac{1}{3}(m-1)^3 + \frac{1}{2}(m-1)^2 + \frac{1}{6}(m-1)$, the variance of W_n is

$$\operatorname{Var}(W_n) = n \operatorname{Var}(\zeta_1) = n\left(\frac{p}{A_0}K(A_0) + \frac{1-p}{A_1}K(A_1) - D^2\right).$$

Comparing this formula with our numerical experiments provides overwhelming evidence for the relationship $\operatorname{Var}(W_n) = \operatorname{Var}(V_n)$. Using the values $p = \frac{4}{7}$ and $D = \frac{5}{7}$ obtained from Example 1, the formula above gives $\frac{1}{n}\operatorname{Var}(W_n) = \frac{24}{49}$.

2.4. **Sensitivity on the initial condition.** Let us next consider the Lyapunov exponent

$$\lambda = \lim_{n\to\infty} \frac{1}{n} \ln \frac{dv_n}{dx} = \lim_{n\to\infty} \frac{1}{n} \sum_{k=1}^{n} \ln \frac{dv_k}{dv_{k-1}}$$

which measures the exponential rate at which two nearby initial points drift apart under the dynamics. Above, the chain rule has been used. Recall the notation introduced in (2) and that $v_0 = x_0 = x$. As $v_k = v_{k-1} + \left(A_{\omega(V_{k-1})} - 1\right) x_{k-1}$,

$$\frac{dv_k}{dv_{k-1}} = 1 + \frac{dA_{\omega(V_{k-1})}}{dv_{k-1}} x_{k-1} + \left(A_{\omega(V_{k-1})} - 1\right) \frac{dx_{k-1}}{dv_{k-1}}.$$

With probability zero v_{k-1} is an integer, in which case $v_{k-1} = V_{k-1}$, $x_{k-1} = 0$, and the process stops. We assume that v_{k-1} is not an integer. Then $\frac{dA_{\omega(V_{k-1})}}{dv_{k-1}} = 0$, $\frac{dx_{k-1}}{dv_{k-1}} = 1$, and $\frac{dv_k}{dv_{k-1}} = A_{\omega(V_{k-1})}$, such that, by (6),

$$\lambda = \lim_{n\to\infty} \frac{1}{n} \sum_{k=1}^{n} \ln A_{\omega(V_{k-1})} = p \ln A_0 + (1-p) \ln A_1$$

and is positive. Roughly speaking, the distance between two very nearby trajectories thus grows like $e^{\lambda n} = \left(A_0^p A_1^{1-p}\right)^n$, which is tantamount to chaos.

2.5. **Numerical study.** The following numerical results are presented in the context of Example 1. However, we have checked that the conclusions also hold for other values of the parameters. In order to study the model introduced above numerically we first create the random tiling (or environment) ω of length $2n+1$ where n is the number of jumps to be performed in a single trajectory. This guarantees that every possible path fits inside the tiling although some computational effort could be saved by choosing the number of tiles closer to $[nD]$. Notice also that while in principle new tiles could be added dynamically to the end of the tiling as required, it is computationally far more efficient to construct the tiling as a static entity in the beginning of the computation.

In practice, the tiling is generated by producing a vector of pseudo-random numbers distributed uniformly on the interval $(0,1)$ using the Mersenne Twister algorithm. The label of the tile $\omega(k)$ is then obtained by rounding the number on each tile k to the nearest integer. The computational tiling $\hat{\omega}$ is finalized by the operation $\hat{\omega}(k) = \omega(k)(A_1 - A_0) + A_0$ yielding a vector whose each element is either A_0 or A_1.

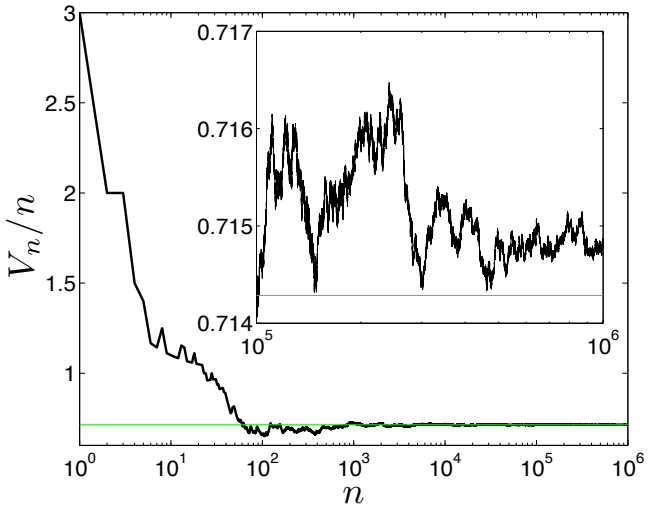

FIGURE 2. Integer part of the position of a particle, V_n, divided by the number of jumps, n, taken for a single typical trajectory. The horizontal line denotes the exact value for the drift $D = 5/7$. The inset shows a blow-up of a part of the main figure.

Each ensemble member (particle trajectory) is initialized by generating a pseudo-random number to determine the starting point $x_0 \in (0, 1)$ of the trajectory. The subsequent particle positions are determined by the underlying tiling. The jumping process could be performed deterministically by keeping track of the exact position v_n of the particle. However, the Markov property of the process provides us a superior way of obtaining the desired statistics stochastically. In this algorithm, before every jump, we sample a new pseudo-random number d from the interval $(0, \hat{\omega}(k))$ depending on the current tile k. Then a jump to the tile $k + [d]$ is made and the whole procedure is repeated n times to produce a single trajectory.

Figure 2 shows a typical trajectory of $n = 10^6$ jumps obtained using the above prescription. The integer part of the position of a particle, V_n, divided by the number of jumps, n, taken is clearly seen to saturate to the analytical value for the drift $D = 5/7$, plotted as a straight line in the figure. The inset shows the late-time evolution of the drift of the particle.

Figure 3 displays the computed probability density function for the random variable $(V_n - nD)/\sqrt{n}$ obtained using 10^7 trajectories of length $n = 10^5$. The solid curve is a normalized Gaussian function with zero mean and variance of $\sigma^2 = 24/49$. Each point in the figure corresponds

to a unique V_n and indicates the relative frequency that a trajectory ends in the corresponding tile after n steps. Joining neighboring points (determined by their abscissae) with lines reveals rapid oscillations in the probability density function. Such lines have been omitted from Figure 3 for the sake of clarity. In the left- and right-hand side insets only trajectories ending in tiles labeled by 0 and 1, respectively, are considered. If the graph in the right-hand side inset is vertically stretched by the factor $\frac{p}{1-p}$, it becomes practically overlapping with the one in the left-hand side inset. This is a consequence of the fact that the fraction of time the particle spends in tiles labeled 0 and 1 is p and $1-p$, respectively. In the figure one can discern several Gaussian shapes, all of which are very well approximated by the analytical Gaussian after normalization with a suitable constant. These "shadow" Gaussians are caused by the quenched environment and they collapse to a single curve if a non-quenched model is used in which A_i is chosen randomly before every jump. The full multi-Gaussian structure of the probability density function is not currently well understood.

Figure 4 shows two cumulative distribution functions, obtained by integrating the numerical and analytical probability densities shown in Figure 3. They match to a great accuracy and we are lead to believe that the random variable $X_n/\sqrt{n} = (v_n - nD)/\sqrt{n}$ is, indeed, normally distributed with zero mean and variance σ^2. We have also analyzed the characteristic function which leads to the same conclusion.

To conclude, our numerical data strongly supports the theoretical analysis presented earlier. Within the numerical accuracy, the distribution is Gaussian with the drift and variance predicted by our analytical calculations. We have performed these numerical experiments using different (fixed) tilings and filling probabilities, p_i, and have always arrived at the same conclusion.

3. Two-dimensional model: hyperbolic toral automorphisms

3.1. **Preliminaries.** We begin by tiling the first quadrant of the plane by unit squares, attaching the label 0 or 1 to each tile. That is, corresponding to each vector $k = (k_1, k_2) \in \mathbb{N}^2$ the tile $[k_1, k_1+1)\times[k_2, k_2+1)$ carries a label $\omega(k) \in \{0, 1\}$. The fixed tiling $\omega = (\omega(k))_{k\in\mathbb{N}^2}$ is our environment and $\mathbb{P}_{p_0}$ stands for the Bernoulli probability measure on the space of such tilings.

The process v_n takes place on the plane and each A_i $(i = 0, 1)$ is a matrix with positive integer entries and determinant 1. Such a matrix

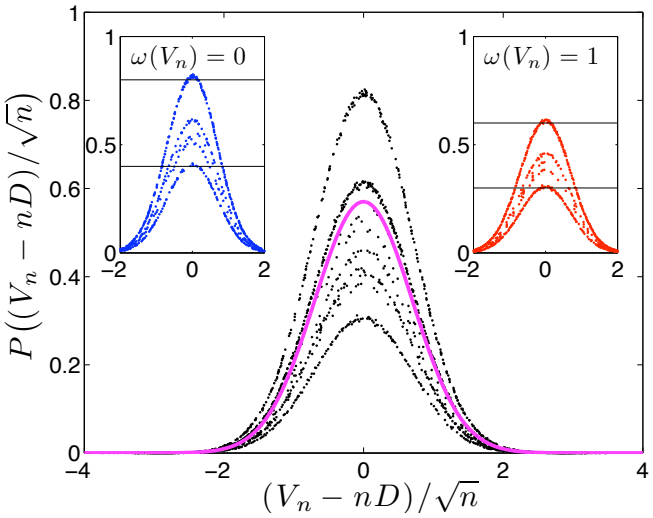

FIGURE 3. Probability density of the random variable $(V_n - nD)/\sqrt{n}$. The solid curve is the Gaussian with zero mean and variance $\sigma^2 = 24/49$. The insets in the left- and right-hand sides show the probability densities for the subsets of trajectories ending to a tile labeled by 0 and 1, respectively. The horizontal lines at levels 0.4, 0.8, 0.3 and 0.6 in the insets are plotted to guide the eye.

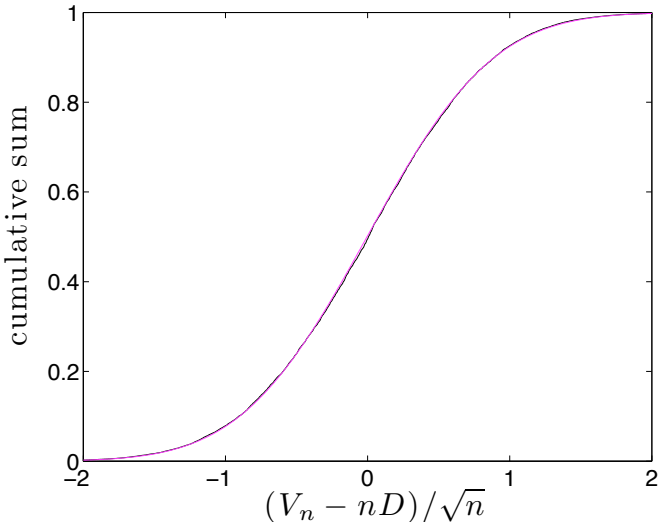

FIGURE 4. Cumulative distribution function corresponding to the data shown in Figure 3. The two curves shown (computational and analytical) are overlapping.

is hyperbolic, with two eigenvalues, $\lambda > 1$ and λ^{-1}, and the eigenvector corresponding to λ points into the first quadrant. The formula $T_i x = A_i x \mod 1$ defines a hyperbolic toral automorphism. A precise description of the dynamics is given by the map on $\mathbb{R}^2_+ \times \mathbb{T}^2$ defined by $(v_{n+1}, x_{n+1}) = (v_n + A_{\omega([v_n])} x_n - x_n, T_{\omega([v_n])}(x_n))$, where $[v_n]$ is the integer part of v_n. The initial condition is $(v_0, x_0) = (x, x)$, with $x \in [0,1)^2$. Let $\mathbf{P}$ denote the Lebesgue measure (*i.e.*, the uniform probability distribution) on the torus $\mathbb{T}^2$ and $\mathbf{E}$ the corresponding expectation.

Example 2. *A concrete example is obtained by choosing* $A_0 = \left(\begin{smallmatrix} 2 & 1 \\ 1 & 1 \end{smallmatrix}\right)$, $A_1 = \left(\begin{smallmatrix} 3 & 1 \\ 2 & 1 \end{smallmatrix}\right)$, *and* $p_0 = p_1 = \frac{1}{2}$.

We claim that the limit

$$D = \mathbf{E}\left(\lim_{n\to\infty} \frac{v_n(x)}{n} \right) = \lim_{n\to\infty} \frac{1}{n} \mathbf{E}(v_n(x)) \,,$$

called the drift, exists and that the (asymptotically) centered random vector

$$Z_n = (X_n, Y_n) = v_n - nD,$$

which measures the fluctuations of v_n relative to the linear drift, is approximately Gaussian with covariance matrix $n\sigma^2$. More precisely, $\frac{1}{\sqrt{n}} Z_n$ converges in distribution to $\mathcal{N}(0, \sigma^2)$, where σ^2 is given by $\lim_{n\to\infty} \mathrm{Cov}\left(\frac{1}{\sqrt{n}} Z_n, \frac{1}{\sqrt{n}} Z_n \right)$: denoting $E_z = (-\infty, z_1] \times (-\infty, z_2]$ for any fixed $z = (z_1, z_2) \in \mathbb{R}^2$,

$$\lim_{n\to\infty} \mathbf{P}\left(\frac{1}{\sqrt{n}} X_n \le z_1, \frac{1}{\sqrt{n}} Y_n \le z_2 \right) = \frac{1}{2\pi\sqrt{\det \sigma^2}} \int_{E_z} e^{-\frac{1}{2} s \cdot (\sigma^2)^{-1} s} \, d^2 s.$$

In contrast with the one-dimensional case, the tiling is *not* a Markov partition for the maps, which considerably complicates the analysis of the model.

3.2. **Drift.** Let us continue to denote $V_n = [v_n]$. We conjecture that the drift vector $D = \left(\begin{smallmatrix} d_1 \\ d_2 \end{smallmatrix}\right)$ is given by

$$D = pD_0 + (1-p)D_1,$$

where $D_i = \mathbf{E}(A_i x - x) = (A_i - \mathbb{1}) \left(\begin{smallmatrix} \frac{1}{2} \\ \frac{1}{2} \end{smallmatrix}\right)$ equals the average jump under the action of the matrix A_i and p is as in (6). The value of p is obtained, as above (5), from an effective transition matrix α^*. Its general element α^*_{ij} is the conditional probability $\mathbf{P} \times \mathbb{P}_{p_0}(\omega(V_1) = j \,|\, \omega(V_0) = i) = \mathbf{P} \times \mathbb{P}_{p_0}(\omega([A_i x]) = j \,|\, \omega(0,0) = i)$—the probability of jumping to a tile labeled j when the initial tile is labeled i and when the choice of the tiling is being averaged out.

In practice, α^*_{ij} is computed as follows. We assume that the initial tile is labeled i, *i.e.*, $\omega(0,0) = i$. The image of the unit square under A_i is a parallelogram of area one that overlaps with various tiles. The area of intersection of the parallelogram with a tile represents the probability of jumping to that tile. α^*_{ij} can then be computed recalling that each tile is labeled 0 with probability p_0 independently of the others. In the case of Example 2, we obtain $D_0 = \begin{pmatrix} \frac{1}{1} \\ \frac{1}{2} \end{pmatrix}$, $D_1 = \begin{pmatrix} \frac{3}{2} \\ 1 \end{pmatrix}$, and $\alpha^* = \begin{pmatrix} \frac{1}{4}+\frac{3}{4}\frac{1}{2} & \frac{3}{4}\frac{1}{2} \\ \frac{5}{6}\frac{1}{2} & \frac{1}{6}+\frac{5}{6}\frac{1}{2} \end{pmatrix} = \begin{pmatrix} \frac{5}{8} & \frac{3}{8} \\ \frac{5}{12} & \frac{7}{12} \end{pmatrix}$, which results in $p = \frac{10}{19}$ and $D = \begin{pmatrix} \frac{47}{38} \\ \frac{14}{19} \end{pmatrix}$.

3.3. **Numerical study.** As mentioned earlier, the Markov property deployed in the numerical study of the one-dimensional problem where we used a stochastic jumping algorithm does not, unfortunately, apply in the two-dimensional case. Instead, we are forced to compute the particle trajectories fully deterministically which renders the numerical problem difficult. Due to the chaotic nature of the process, the position v_n of the particle must now be represented with an accuracy to approximately $2n$ decimal places in order to keep the accumulation of the numerical rounding errors bounded. This must be done using a software implementation since the double precision float native to the hardware only contains 15 decimal places.

We first create the tiling ω as in the one-dimensional case with the exception that it is now a two-dimensional object. We then choose randomly the initial position of the particle within the unit square. The label $\omega(0,0)$ of the initial tile is then read and the new position of the particle is computed by applying the corresponding map $T_{\omega([v])}$. This jumping procedure is repeated n times. The time to compute a single trajectory increases dramatically as the path length n is increased due to the corresponding increase in the required accuracy of the representation of the position of the particle.

Figure 5 shows the convergence of the drifts D_i and that of the covariance matrix elements σ^2_{ij}. The values in descending order at $n = 10^3$ are d_1, d_2 , σ^2_{11}, $\sigma^2_{12} = \sigma^2_{21}$, and σ^2_{22}. The straight lines indicate the analytical values for the drift components. Each data point is composed using 10^4 trajectories.

In Figure 6 (a)–(c) we have plotted the particle positions in the plane after $n = 1, 2, 3$, and 2000 jumps, respectively. The trajectories were initiated randomly from the unit square. The straight diagonal lines indicate the direction of the drift and the cross in frame (d) denotes the directions of the eigenvectors of the covariance matrix. Since the initial tile in our environment had the label $\omega(0,0) = 1$, the frame (a) simply shows how A_1 maps the unit square. The subsequent jumps

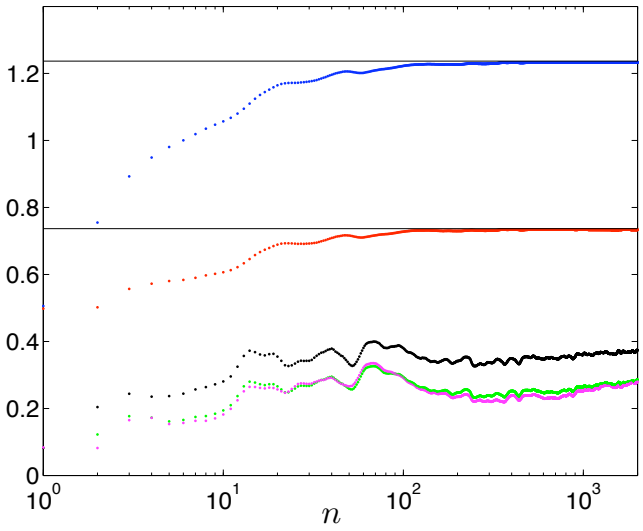

FIGURE 5. Values for the x and y components of the drift and the covariance matrix elements σ_{11}^2, $\sigma_{12}^2 = \sigma_{21}^2$, and σ_{22}^2 as a function of n, respectively, in descending order at $n = 1000$. The straight lines indicate the analytical values of drift components d_1 and d_1.

shred the distribution, as illustrated by the frames (b) and (c), because particles in different tiles undergo different transformations. Figure 7 shows a contour plot of the particle distribution after $n = 100$ jumps and reveals prominent stripes, due to the shredding, which are roughly aligned with the direction of the drift vector.

Figure 8 shows the probability density of $\frac{1}{\sqrt{n}}Z_n$ obtained after $n = 2000$ jumps. Embedded is also a two-dimensional Gaussian probability density which has the same covariance matrix as the numerical data. Despite of the fact that the density function itself does not converge to any function, the corresponding cumulative distribution function shown in Figure 9 is smooth and matches that of the corresponding Gaussian distribution. The maximum absolute difference between the numerical and analytical functions is 0.017, most of which is due to the highest peak in Figure 8.

4. CONCLUSIONS

We have investigated the statistical properties of a deterministic walk in a quenched one-dimensional random environment of expanding circle maps and have analytically found the drift and variance for the

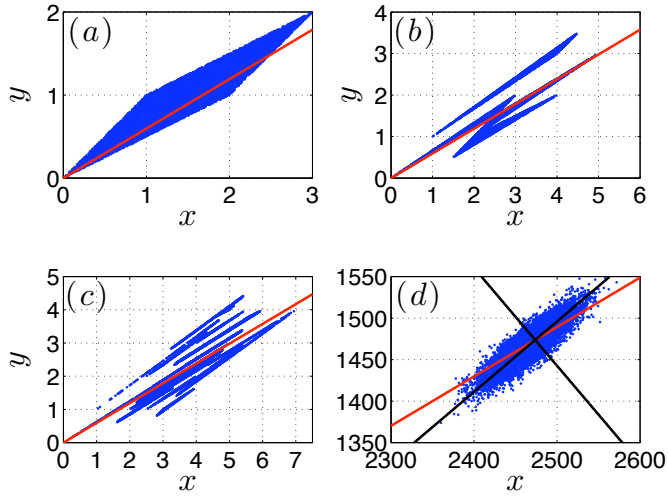

FIGURE 6. End points v_n of 10^4 trajectories in the plane after $n = 1$ (a), $n = 2$ (b), $n = 3$ (c), and $n = 2000$ (d) jumps. The straight diagonal lines trace the drift vector and the cross in frame (d) shows the eigendirections of the covariance matrix. Each frame comprises 10000 data points.

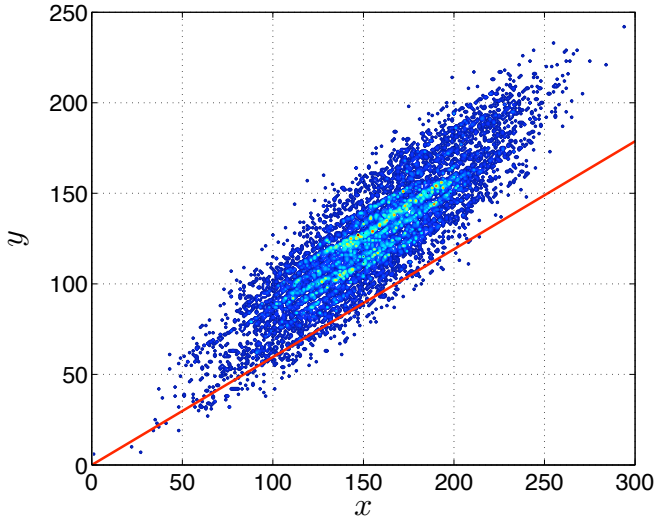

FIGURE 7. Contour plot of the particle distribution in the plane after $n = 100$ jumps. The straight line shows the direction of the drift vector.

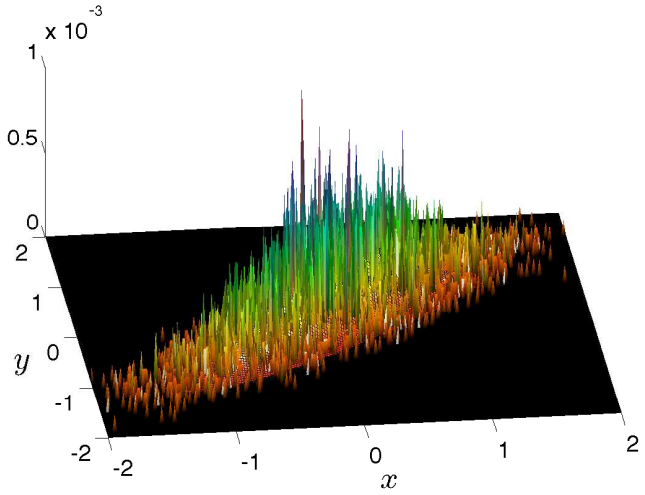

FIGURE 8. Probability density function for the random variable $Z_n/\sqrt{n}$. The spikes are an inherent feature of the distribution and the density does not converge to any function. Embedded is the analytical Gaussian function.

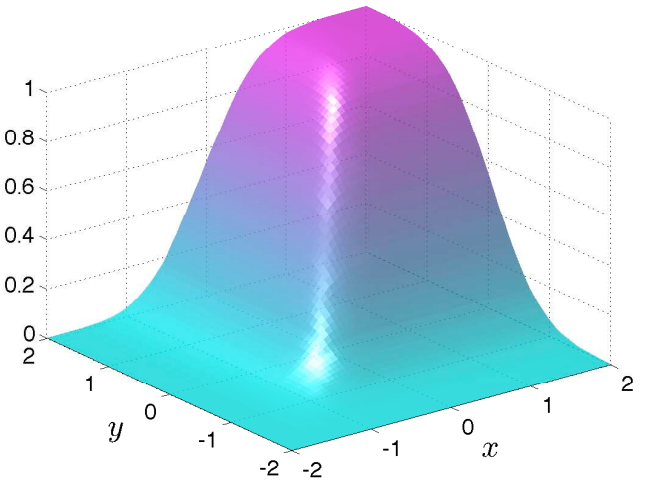

FIGURE 9. Cumulative distribution function corresponding to the data shown in Figure 8.

resulting Gaussian probability distribution. Using numerical experiments we have been able to verify our analytical predictions. We have further studied a two-dimensional model similar to the one-dimensional system where hyperbolic toral automorphisms take the place of the circle maps. Again the probability distribution turns out to be Gaussian

with certain linear drift and covariance. The key feature and complicating factor in both the one- and two-dimensional cases is the *fixed* random environment. A direct consequence of this is that, even after the proper scaling, the probability density does not converge to any function—a result which persists both in our one- and two-dimensional models. The implementation of recurrence to this model will be left for future work.

References

[AySt] A. Ayyer and M. Stenlund, *Exponential Decay of Correlations for Randomly Chosen Hyperbolic Toral Automorphisms*, Chaos, **17** (2007), 043116.

[AyLiSt] A. Ayyer, C. Liverani, and M. Stenlund, *Quenched CLT for Random Toral Automorphism*, To appear in Discrete and Continuous Dynamical Systems A.

[BuSi] L. A. Bunimovich and Ya. G. Sinai, *Statistical properties of Lorentz gas with periodic conguration of scatterers*, Comm. Math. Phys. **78** (1980/81), no. 4, 479–497.

[ChDo] N. I. Chernov and D. Dolgopyat, *Hyperbolic billiards and statistical physics*, ICM 2006 Proceedings.

[ChMa] N. I. Chernov and R. Markarian, *Chaotic Billiards*, AMS, 2006.

[Lo] H. A. Lorentz, *The motion of electrons in metallic bodies I, II, and III*, Koninklijke Akademie van Wetenschappen te Amsterdam, Section of Sciences, 7 (1905).

[Si] Ya. Sinai, *Dynamical systems with elastic reflections*, Russ. Math. Surv. **25**, (1970).

[Sz] *Hard ball systems and the Lorentz gas*, ed. D. Szász, Springer-Verlag, 2000.

[Ta] S. Tabachnikov, *Billiards*, Société Mathématique de France, Paris, 1995.

E-mail address: tapio.simula@gmail.com

(Tapio Simula) Mathematical Physics Laboratory, Department of Physics, Okayama University, Okayama 700-8530, Japan.

E-mail address: mikko@cims.nyu.edu

(Mikko Stenlund) Courant Institute of Mathematical Sciences, New York, NY 10012, USA; Department of Mathematics and Statistics, P.O. Box 68, Fin-00014 University of Helsinki, Finland.

URL: http://www.math.helsinki.fi/mathphys/mikko.html